

Demonstration of a refractometric sensor based on optical microfiber coil resonator

Fei Xu^{a)} and Gilberto Brambilla

Optoelectronics Research Centre, University of Southampton, Southampton SO17 1BJ, United Kingdom

(Received 30 October 2007; accepted 25 February 2008; published online 14 March 2008)

We experimentally demonstrated a refractometric sensor based on a coated optical microfiber coil resonator. It is robust, compact, and comprises an intrinsic fluidic channel. A sensitivity of about 40 nm/RIU (refractive index unit) has been measured, in agreement with predictions. © 2008 American Institute of Physics. [DOI: 10.1063/1.2898211]

Evanescent-field-based optical resonators in the form of microspheres, photonic crystals, microdisks, microtoroids, and microrings have been under intensive investigation for deployment as biological and/or chemical sensors.^{1–9} Resonating structures can provide a simple, inexpensive, high-throughput technology for label-free real-time measurements and are attracting increasing interest. Subwavelength-diameter optical microfibers are ideal sensor elements because of their low cost, low loss, and very large evanescent fields.^{10–13} Microfiber resonators, in the form of loop and multicoils, have the advantage of a launching/collection efficiency close to unity thanks to their extremities fiber pigtailed. Thus, microfiber resonators do not suffer the onerous input/output coupling problems experienced by other high- Q (quality factor) resonators. The remaining dominating problem, associated with devices based on microfiber resonators, is the temporal degradation of their optical and mechanical properties when manufactured in air.¹³ This issue was resolved by embedding the devices and this has led to the proposal to develop several high sensitivity sensors^{14,15} based on microfiber coil resonators.^{16–18} Although they are protected by a layer of coating, they still have a large evanescent field. Three-dimensional (3D) microfiber microcoil resonators have been experimentally demonstrated by wrapping microfibers on a rod¹⁹ and coating them with Teflon²⁰ or immersing them in a low refractive index liquid.²¹ The optical microfiber coil refractometric sensor (OMCRS) has been obtained from an embedded 3D microfiber microcoil resonator by removing its supporting rod. The proposed OMCRS has a microfluidic channel for the analyte delivery and has small size, high sensitivity, high selectivity, and low detection limits. It is also strong and portable because it is coated and embedded in a polymeric host.

In this letter, we experimentally demonstrate an OMCRS based on a Teflon-coated 3D microfiber coil resonator.

The OMCRS was fabricated as follows. First, a microfiber was fabricated with the so-called modified flame-brushing technology using the setup presented in Ref. 22 with a microheater (NTT-AT, Japan). The length and diameter of the uniform waist region of the fabricated microfiber were 50 mm and $\sim 2.5 \mu\text{m}$, respectively. The microfiber was then wrapped on a 1 mm diameter polymethylmethacrylate (PMMA) rod. PMMA is a polymer with an amorphous structure which is soluble in acetone, has a density of 1.19 g/cm^3 ,

very low water absorption, and a refractive index in the range of 1.49–1.51. The whole structure was repeatedly coated by the Teflon solution 601S1-100-6 (DuPont, USA), in order to form a protective embedding layer that was as thick as possible. The overall drying time in air depends on the number and thickness of the embedding Teflon layers and it is in the range of hours. The dried embedded microcoil resonator was then left soaking into acetone to dissolve the support rod. The whole PMMA rod was completely dissolved in 1–2 days at room temperature. Finally, the OMCRS sensor with a $\sim 1 \text{ mm}$ diameter microchannel and two input/output pigtailed was obtained. The picture of the sensor is shown in Fig. 1. The sensor consists of a microfiber resonator with five turns and has a microfluidic channel inside. The adjacent microfibers are very close and the major coupling area is in the middle. Although some bubbles are left inside the OMCRS during the drying process, these seem to be far from the microfiber and do not affect the overall sensor operation.

Even though the transmission properties of a multiturn microfiber coil resonator can be simulated by solving multiple coupled wave equations, its spectrum is very complicated. In most cases, there is only one dominating resonance, which can be easily evaluated using the coupled mode equations with results analogous to those of a single-loop resonator;²³ if $\beta = 2\pi n_{\text{eff}}/\lambda$ is the propagation constant, n_{eff} effective index, α the loss coefficient, K coupling parameter, and length L of a single turn, then T can be written as²⁴

$$T = \frac{\exp(i\beta L - \alpha L) - \sin K}{1 - \exp(-i\beta L + \alpha L)\sin K}. \quad (1)$$

Resonances in T occur if K and β are near to values



FIG. 1. (Color online) Picture of the OMCRS.

^{a)}Tel.: +44 (0) 23 8059 9254. FAX: +44 (0) 23 8059 3149. Electronic mail: feix@orc.soton.ac.uk.

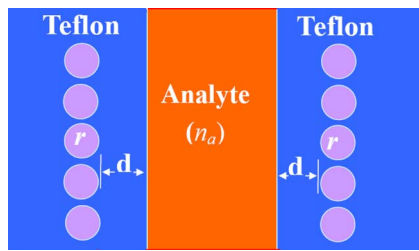


FIG. 2. (Color online) Schematic of the cross section of an OMCRS.

$$K_m = \frac{\pi}{2}(2m + 1), \quad m = 1, 2, \dots, \quad (2)$$

$$\beta_m = \pi(2n + m) \quad \text{where } n \text{ is an integer}, \quad (3)$$

respectively.

From Eqs. (1)–(3), it is clear that the wavelength at resonance changes with n_{eff} .

Figure 2 shows a schematic of the OMCRS cross section. Because of the interface with the analyte, the mode propagating in the coated microfiber experiences a refractive index surrounding similar to that of a conventional D-shaped fiber.^{25,26} The mode properties are particularly affected by two parameters: the microfiber radius r and the coating thickness d between the microfiber and the fluidic channel. We evaluated the effective index n_{eff} of the fundamental mode propagating in the optical microfiber by a finite element method with the commercial software COMSOL3.3. The fundamental mode is the one with the largest propagation constant and the only mode that is well confined in the vicinity of the microfiber.^{25,26} Generally, n_{eff} increases as the analyte refractive index (n_a) increases, and increases more sharply for smaller d because in this case a larger fraction of the mode is propagating in the analyte. In the OMCRS we fabricated $d \sim 0$.

The performance of resonant refractive index sensors can be evaluated by using the sensitivity S , which is defined as the magnitude in shift of the resonant wavelength divided by the change in refractive index of the analyte.²⁷

The sensitivity was measured by inserting the sensor in a beaker containing mixtures of isopropyl and methanol, where the isopropyl component had the following ratios: (1) 60%, (2) 61.5%, (3) 63%, (4) 64.3%, (5) 65.5%, (6) 66.7%, and (7) 67.7%. These solutions were chosen with the objective of simulating aqueous solutions, having a refractive index in the region around 1.33 at a wavelength of $\lambda = 1.55 \mu\text{m}$. The ratio was increased by adding small calibrated quantities of isopropyl to the solution at a position far from the sensor. The refractive indexes of pure isopropyl and methanol at $1.5 \mu\text{m}$ are 1.364 and 1.317, respectively.²⁸ The sensor was connected to an erbium-doped fiber amplifier and an optical spectrum analyzer and then immersed into the mixtures. Figure 3 shows the spectra recorded at 1530 nm. The resonator peak shifts towards longer wavelengths for increasing mixture refractive indexes. These results agree with our predictions from Eqs. (1)–(3). Due to the change in the overlap between the mode propagating in the resonator and the analyte, an increase in n_a produces an increase in n_{eff} and thus in the resonator peak wavelength. In contrast, the extinction ratio does not behave in a linear fashion. It increases with increasing n_a from (1) to (4), where it achieves a maximum, and then decreases for further increases of n_a .

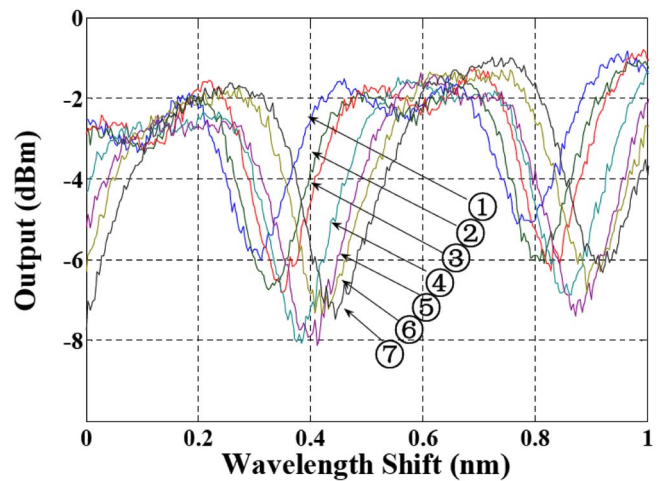


FIG. 3. (Color online) Output spectrum of the OMCRS in seven different mixtures of isopropyl of methanol. The Isopropyl fraction is (1) 60%, (2) 61.5%, (3) 63%, (4) 64.3%, (5) 65.5%, (6) 66.7%, and (7) 67.7%, respectively.

This can be explained by the change of the coupling coefficient with the refractive index. The coupling coefficient has a strong periodical dependence on the refractive index and, hence, a small change in n_a can induce a significant, nonlinear change in the coupling coefficient, and thus in T through Eq. (1). Figure 4 shows the measured wavelength shift (dashed lines) and calculated (solid lines) for $r = 1250 \text{ nm}$ and different polymer thicknesses d . The simulation shows that the best fit occurs for $d \sim 0$, in agreement with the experimental results. The small difference observed in Fig. 4 has been attributed to the uneven profile of the microfiber diameter, to the imprecise winding of the microcoil resonator, to the roughness of the channel inner surface, and to the uneven distance of the microfiber from the microfluidic channel. The sensitivity, defined as the slope of these lines,²⁷ was evaluated to be about 40 nm/RIU (refractive index unit) from the data of Fig. 4. This value is comparable with those reported previously for microsphere and microring resonators,^{2,4,5} but smaller than recently reported values for a slot waveguide (212.13 nm/RIU) (Ref. 29) and for a liquid core resonator (800 nm/RIU).³⁰ The relatively low value for the sensitivity can be attributed to the small overlap between the mode propagating in the microfiber resonator and the

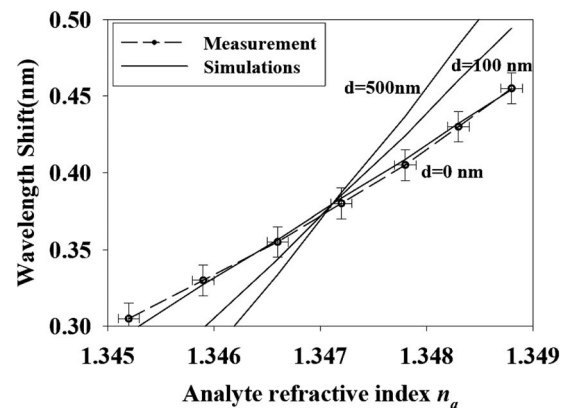


FIG. 4. Dependence of the measured and calculated wavelength shifts on the liquid mixture refractive index. The dashed line represents the measured results while the solid lines are the calculated results for $r = 1250 \text{ nm}$ and different polymer thicknesses d .

analyte. Another factor which has probably affected the sensor sensitivity is the lack of smoothness of the device surface in contact with the analyte. This is possibly caused by PMMA residues on the surface of the channel or it may originate from the original roughness of the PMMA support rod. This roughness produced the moderately low Q factor observed in the resonator ($Q \sim 10^4$), which limited the interaction length between the mode and the analyte. We forecast that the overall sensitivity can be considerably improved to $\sim 10^4$ by using thinner microfibers and by fabricating micro-coil resonators with higher Q factors.

In summary, a refractometric sensor based on a microfiber coil resonator was experimentally demonstrated and a sensitivity of about 40 nm/RIU was recorded. High sensitivities can be achieved by improving the manufacturing technology.

The authors gratefully acknowledge the help of Dr. N. Broderick with the software package COMSOL, initiating discussions with Professor D. J. Richardson, and financial support by the EPSRC. G.B. thanks the Royal Society (London, U.K.) for his Research Fellowship.

¹R. W. Boyd and J. E. Heebner, *Appl. Opt.* **40**, 5742 (2001).

²M. Adams, G. A. DeRose, M. Loncar, and A. Scherer, *J. Vac. Sci. Technol. B* **23**, 3168 (2005).

³C. Y. Chao, W. Fung, and L. J. Guo, *IEEE J. Sel. Top. Quantum Electron.* **12**, 134 (2006).

⁴N. M. Hanumegowda, C. J. Stica, B. C. Patel, I. White, and X. D. Fan, *Appl. Phys. Lett.* **87**, 201107 (2005).

⁵I. M. White, H. Oveys, X. Fan, T. L. Smith, and J. Y. Zhang, *Appl. Phys. Lett.* **89**, 191106 (2006).

⁶I. M. White, H. Y. Zhu, J. D. Suter, N. M. Hanumegowda, H. Oveys, M. Zourob, and X. D. Fan, *IEEE Sens. J.* **7**, 28 (2007).

⁷I. M. White, N. M. Hanumegowda, and X. Fan, *Opt. Lett.* **30**, 3189 (2005).

⁸A. M. Armani and K. J. Vahala, *Opt. Lett.* **31**, 1896 (2006).

⁹K. J. Vahala, *Nature (London)* **424**, 839 (2003).

¹⁰L. M. Tong, J. Y. Lou, and E. Mazur, *Opt. Express* **12**, 1025 (2004).

¹¹S. G. Leon-Saval, T. A. Birks, W. J. Wadsworth, P. S. J. Russell, and M. W. Mason, *Opt. Express* **12**, 2864 (2004).

¹²G. Brambilla, V. Finazzi, and D. J. Richardson, *Opt. Express* **12**, 2258 (2004).

¹³G. Brambilla, F. Xu, and X. Feng, *Electron. Lett.* **42**, 517 (2006).

¹⁴F. Xu, P. Horak, and G. Brambilla, *Opt. Express* **15**, 7888 (2007).

¹⁵F. Xu, V. Pruneri, V. Finazzi, and G. Brambilla, *Opt. Express* **16**, 1062 (2008).

¹⁶M. Sumetsky, *Opt. Express* **12**, 2303 (2004).

¹⁷F. Xu, P. Horak, and G. Brambilla, *Appl. Opt.* **46**, 570 (2007).

¹⁸F. Xu, P. Horak, and G. Brambilla, *J. Lightwave Technol.* **25**, 1561 (2007).

¹⁹F. Xu and G. Brambilla, *IEEE Photonics Technol. Lett.* **19**, 1481 (2007).

²⁰F. Xu and G. Brambilla, *Opt. Lett.* **32**, 2164 (2007).

²¹M. Sumetsky, Optical Fiber Communication Conference, San Diego, USA, 2007 (unpublished).

²²G. Brambilla, E. Koizumi, X. Feng, and D. J. Richardson, *Electron. Lett.* **41**, 400 (2005).

²³M. Sumetsky, Y. Dulashko, J. M. Fini, A. Hale, and D. J. DiGiovanni, *J. Lightwave Technol.* **24**, 242 (2006).

²⁴M. Sumetsky, Y. Dulashko, J. M. Fini, and A. Hale, *Appl. Phys. Lett.* **86**, 161108 (2005).

²⁵D. Marcuse, F. Ladouceur, and J. D. Love, *IEEE Proc.-J: Optoelectron.* **139**, 117 (1992).

²⁶M. S. Dinleyici and D. B. Patterson, *J. Lightwave Technol.* **15**, 2316 (1997).

²⁷I. M. White and X. Fan, *Opt. Express* **16**, 1020 (2008).

²⁸C. B. Kim and C. B. Su, *Meas. Sci. Technol.* **15**, 1683 (2004).

²⁹C. A. Barrios, K. B. Gylfason, B. Sanchez, A. Griol, H. Sohlstr, M. Hologado, and R. Casquel, *Opt. Lett.* **32**, 3080 (2007).

³⁰M. Sumetsky, R. S. Windeler, Y. Dulashko, and X. Fan, *Opt. Express* **15**, 14376 (2007).